

See discussions, stats, and author profiles for this publication at: <https://www.researchgate.net/publication/41406761>

Spatially Resolved Quantification of E-Cadherin on Target hES Cells

ARTICLE *in* THE JOURNAL OF PHYSICAL CHEMISTRY B · MARCH 2010

Impact Factor: 3.3 · DOI: 10.1021/jp906737q · Source: PubMed

CITATIONS

15

READS

12

7 AUTHORS, INCLUDING:



Indumathi Sridharan
Illinois Institute of Technology

7 PUBLICATIONS 87 CITATIONS

[SEE PROFILE](#)



Honghong Zhang
Illinois Institute of Technology

8 PUBLICATIONS 42 CITATIONS

[SEE PROFILE](#)



Rong Wang
Illinois Institute of Technology

55 PUBLICATIONS 4,462 CITATIONS

[SEE PROFILE](#)

Spatially Resolved Quantification of E-Cadherin on Target hES Cells

Zhaoxia Li,[†] Dengli Qiu,[†] Indumathi Sridharan,[†] Xiaoping Qian,[‡] Honghong Zhang,[†] Chunbo Zhang,[†] and Rong Wang^{*,†}

Department of Biological, Chemical, and Physical Sciences and Department of Mechanical, Materials, and Aerospace Engineering, Illinois Institute of Technology, Chicago, Illinois 60616

Received: July 16, 2009; Revised Manuscript Received: December 9, 2009

The local expression and distribution pattern of protein on a cell play essential roles in signal transduction within a cell or between cells. Here we report on the development of a spatially resolved quantification method, which was applied in the study of E-cadherin local expression in identified undifferentiated and differentiated human embryonic stem (hES) cells in their native cellular environment. This was achieved by a novel immunofluorescence assisted affinity mapping (IF-AM) method, in which immunofluorescence provides the guidance to locate a desired type of cell in a cell community for performing affinity mapping to quantify the local protein density. The results unveiled the crucial role of E-cadherin in mediating hES cell proliferation and differentiation: the expression of E-cadherin is markedly higher on undifferentiated cells, and the growth of hES cells in unique colonies is contingent on the homogeneous distribution of E-cadherin. Due to the ability of directly assessing individual proteins of a cell, the IF-AM method is shown to be a sensitive tool for resolving subtle differences in the local expression of membrane proteins even at low abundance.

Introduction

Quantification of the local expression level of a surface protein on a selected single cell in the context of its native environment is essential for unveiling the signal transduction cascades within a cell or between cells. Many approaches, such as immunohistochemistry,¹ electron microscopy,² and fluorescent molecule or particle based imaging tools,³ have demonstrated the capability of quantifying certain protein expression levels in a cell. However, these methods rely on the interactions between labeled antibody and antigen or labeled ligand and receptor in a bulk solution. Due to the intrinsic limitations of diffusion controlled processes and the requirement of subsequent washing, these methods can provide the relative quantification of proteins; however, they are not precise for analyzing low-abundant proteins. Methods that can perform absolute quantification of protein expression in a cell are highly desirable for probing low-abundant proteins at high sensitivity.

In many cases, the target cells are the side population cells in a complex cell community, thus the ability to quantify proteins against a single specific cell is critical to understanding cell–cell interactions in the complex community. Several methods, such as flow cytometry,^{4,5} patch-clamp aspiration,^{6,7} and laser capture microdissection,^{8,9} are available for picking a particular cell out of a cell culture for follow-up quantitative analysis at the single cell level. However, information concerning physical location of proteins and cells in the cellular environment is lacking. A cell function is pertinent to its communication with surrounding cells and the collective behavior of proteins in their native environments. Therefore, quantitative analysis of proteins in the context of their physical locations in subcellular and cellular environments is imperative.

Atomic force microscopy (AFM) has been increasingly adopted in biomolecular and cellular investigations due to its

ability to directly “see” individual proteins or DNA in motion.¹⁰ Single-molecule force spectroscopy has opened unique opportunities to manipulate proteins at the single molecule level while examining their structural and conformational changes.^{10–12} In principle, the method can be applied to the study of membrane proteins in cells by “seeing” the individual proteins and counting the protein numbers. However, the application was mostly demonstrated on simplified substrates, such as purified proteins or isolated cytoplasmic membranes containing dense and highly ordered protein arrays on glass or mica. A cell membrane is rough, soft, and complex due to the diverse distribution of various cell-surface proteins and phospholipids. Affinity mapping utilizes an antibody modified tip to scan a cell membrane pixel by pixel to detect the target protein via specific binding force measurements.^{13–17} Although this method also relies on the interactions between labeled antibody and antigen or labeled ligand and receptor, due to the direct “touch” approach, the local concentration of antibody or ligand is sufficiently high. This warrants the specific interaction between the counter proteins on the tip and on the cell membrane and consequently warrants the absolute quantification of both high and low abundant proteins.

Cells belonging to different populations coexist in a complex tissue. In light of the fluorescence-AFM imaging approach,^{18,19} we developed an immunofluorescence assisted affinity mapping (IF-AM) method for probing the protein expression and distribution pattern on a cell from an identified population. We pursued a strategy of tracing the biomarker fluorescence to locate a target cell within a cell community and performed *in situ* affinity mapping by AFM to identify the protein species and evaluate protein distribution without physically disturbing the cells. We further enhanced the method by quantifying the protein density at a local region of a cell, which can potentially be applied in on-site cell sorting/screening.

We applied this method to the study of human embryonic stem (hES) cells. One feature of hES cells is that undifferentiated cells maintain their “stemness” in a colony format; any cells

* To whom correspondence should be addressed. E-mail: wangr@iit.edu.
Tel.: 312-567-3121. Fax: 312-567-3494.

[†] Department of Biological, Chemical, and Physical Sciences.

[‡] Department of Mechanical, Materials, and Aerospace Engineering.

departing from colonies are subjected to differentiation.^{20–22} Because a compact colony contains thousands of cells, cell–cell interaction may play an important role in colony expansion (i.e., proliferation) and stem cell differentiation. E-Cadherin is the major adhesion protein which dictates the cell–cell interactions and regulates many signaling pathways in making cell fate decisions.^{23–25} Here, we attempted the quantification of the local expression of E-cadherin on undifferentiated and spontaneously differentiated hES cells using the IF-AM method. The results suggest that E-cadherin is abundant and homogeneously distributed on undifferentiated cells, favoring the multilayer growth of cells in developing colonies. Its expression is 2- to 16-fold lower on differentiated cells, depending on the cell lineage. We also studied, in parallel, TRA-1-81, a hES cell marker membrane protein for undifferentiated hES cells. Its heterogeneous distribution on undifferentiated cells is unique and in contrast to the homogeneous distribution of E-cadherin and thus can be used as a physical marker to identify early differentiation. As can be seen, IF-AM is a sensitive tool for laterally resolving complex and subtle differences in membrane protein local expression.

Experimental Methods

hES Cell Culture. hES cell line H9 was obtained from WiCell (Madison, WI). Cells were routinely cultured on feeder cells derived from mitotically inactivated mouse embryo fibroblasts (MEFs) and were maintained in DMEM/F12 (Mediatech, Herndon, VA) containing 20% knockout serum replacement, 1% nonessential amino acids, 1 mM L-glutamine, 100 μM β-mecaptoethanol, and 4 ng/mL of bFGF (Invitrogen, Carlsbad, CA). The media were changed everyday, and cells were passaged every 6 or 7 days. All cultures were monitored with hES cell undifferentiated markers. For spontaneously differentiated cells, the hES cells were dissociated by 0.25% Trypsin with 2.21 mM EDTA (Invitrogen, Carlsbad CA) to obtain a single-cell suspension, then directly passaged onto a gelatin (Millipore, Philipsburg, NJ) coated culture dish containing DMEM (Mediatech, Herndon, VA) supplemented with 10% fetal bovine serum (Hyclone, Logan, UT) and cultured for up to 13 days for the experiments.

Immunofluorescent Staining. hES cells were fixed and permeabilized with precooled methanol for 7 min at room temperature and incubated with 1% BSA in PBST for 1 h to block the nonspecific binding of antibodies. The cells were then incubated within primary antibodies in 1% BSA in PBST for 2 h at room temperature or 24 h at 4 °C. After three washes with PBS, the cells were incubated with secondary antibodies in 1% BSA for 1 h at room temperature in the dark. The nuclei were then stained with DAPI (Invitrogen, Eugene, OR) for 15 min. The following antibodies and dilutions were used: rabbit anti-Oct-4 (Abcam, Cambridge, MA), 1:100; mouse anti-E-cadherin (Zymed, Carlsbad, CA), 1:50; mouse anti-TRA-1-81 (Millipore, Billerica, MA), 1:50; goat anti-Sox17 (R&D System, Minneapolis, MN), 1:40; goat antibrachyury (R&D System, Minneapolis, MN), 1:40; rabbit anti-β-tubulin (Cell-signaling, Danvers, MA), 1:50; Alexa Flour-488 or Alexa Flour-594 conjugated donkey antimouse or donkey antirabbit (Invitrogen, Carlsbad, CA), 1:200; NL493 conjugated donkey antigoat (R&D System, Minneapolis, MN), 1:200.

Western Blot Analysis. Cultures from undifferentiated hES cells or spontaneously differentiated hES cells were harvested on day 13 and homogenized in RIPA lyses solution (50 mM Tris-HCl pH 7.4, 150 mM NaCl, 0.5% sodium deoxycholate, 0.1% SDS, 1% NP-40) at 4 °C. The supernatant was collected, and the protein concentration was measured using a protein

assay kit (Bio-Rad). Equal amounts of proteins were loaded for SDS-PAGE analysis. Western blot analysis was conducted using antibodies specific for E-cadherin (Zymed) or β-actin (Chemicon) and visualized by enhanced chemiluminescence (Pierce).

Tip Modification. For affinity mapping experiments, Si₃N₄ tips (Veeco, Santa Barbara, CA) were coated with titanium (3 nm thickness) and gold (15 nm thickness) by a thermoevaporator (Denton Vacuum, NJ). Antibodies against E-cadherin or TRA-1-81 (Invitrogen, Carlsbad, CA) were conjugated on the tips via a cross-linker, *N*-succinimidyl 3-(2-pyridyldithio) propionate (SPDP, Molecular Probes, Eugene, OR), as routinely performed in our lab.^{16,26–28} The tips were thoroughly rinsed after each modification step to remove any unbound residues. According to the topographic images of gold-coated silicon wafer functionalized by antibodies under the same conditions, antibodies were uniformly and densely distributed across the surface. The monolayer coverage was evaluated by the 8 ± 1 nm thick protein layer with respect to the bare substrate. Occasionally, physically adsorbed protein clusters were observed on the protein monolayer. The same surface feature is expected on antibody functionalized AFM tips. Physically adsorbed proteins are less stable, hence easily detach from a tip. To ensure the consistency of antibody coverage on tips in all experiments, we chose to use the tips showing reproducible adhesion forces measured at the same sample location in multiple approaching and retraction cycles. This property is an indication of monolayer coverage of covalently bound antibodies. A gold-coated tip was also modified by oligo-ethylene glycol (HSC₁₁-EG₆, ProChimia, Gdansk, Poland) to evaluate the level of nonspecific interaction between the tip and a cell membrane surface.

IF-AM Experimental Setup. A Picoscan 3000 AFM (Agilent technology, Tempe, AZ) was configured with a Nikon TE-U 2000 fluorescence microscope by using a customized sample stage, allowing each sample to be examined by both microscopes. All measurements were performed directly on cells cultured on dishes. The cells were moderately treated by precooled methanol for 7 min, then stained against the undifferentiated or differentiated cell markers for identification of cell type. A chosen cell can be aligned with the AFM tip and cantilever within the visual field of the inverted microscope.

All AFM measurements were carried out at room temperature in fluid contact mode. PBS buffer (pH = 7.4) was used as the medium. The spring constant of functionalized Si₃N₄ tips was calibrated by using reference cantilevers with known spring constants²⁹ and was 0.065 ± 0.008 N/m for all the tips used in the study. When the tip scanned a cell surface, a force spectrum was recorded at each pixel upon tip approaching and retraction. The appearance of an adhesion peak in the retraction curve quantitatively reveals the unbinding of antigen–antibody specific interaction. A homemade Matlab program was used to generate the affinity map based on the maxima of a total of 32 × 32 = 1024 retraction curves in 4 × 4 μm² images. The z-scan rate of the measurements was 0.5 Hz, and the z-ramp size was 3.8 μm.

Results

IF-AM Method. The apparatus of the IF-AM was set by combining a fluorescence microscope with an AFM so that a cell can be examined under both microscopes. We prestained the hES cells on a culture dish with the antibody against Oct-4, a marker of undifferentiated pluripotent hES cells. As shown in Figure 1a, the immunofluorescence directed the AFM tip to an Oct-4 positive cell. The modification of an AFM tip with anti-E-cadherin enabled the tip to distinguish E-cadherin from other membrane species via the antigen–antibody specific

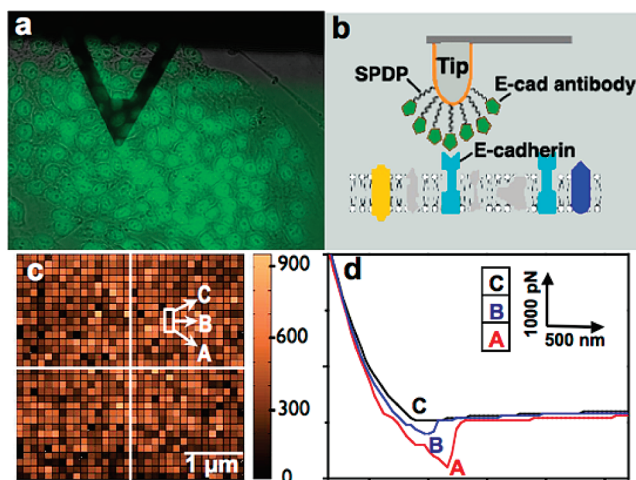


Figure 1. IF-AM study of E-cadherin expression on a hES cell. (a) Merge of phase and immunofluorescent images of undifferentiated hES cells on a cell culture dish. An anti-E-cadherin modified AFM tip is shown to position on an Oct-4 positive (green) cell. (b) Scheme of identifying E-cadherin on a cell membrane using an antibody modified AFM tip. (c) An affinity map reconstructed from a total of 1024 force curves that were collected on the cell in (a) when the anti-E-cadherin modified AFM tip scanned 32 pixels per line at a lateral range of $4 \times 4 \mu\text{m}^2$. (d) Typical force curves acquired at the highlighted pixels in (c).

interaction (Figure 1b) despite the complexity of the cell membrane surface. As the tip scanned the cell surface, a force spectrum was recorded at each pixel. A total of $32 \times 32 = 1024$ force curves were collected (regardless of the scan size) to construct an affinity map as shown in Figure 1c. Figure 1d shows three typical force curves collected at the highlighted pixels in Figure 1c. The bright (A), brown (B), and dark (C) pixels correlate to high (801 pN), medium (440 pN), and low (70 pN) adhesion forces, respectively. Therefore, the contrast of an affinity map highlights the high affinity binding sites, hence the distribution of E-cadherin at a local area. Note that in the z-scan rate range of 0.5–2 Hz and when the z-ramp size was constant, the lower the z-scan rate, the higher the unbinding forces measured. When the scan rate was lower than 0.5 Hz, the unbinding forces remained at the same level as those measured at 0.5 Hz. This implies that the 0.5 Hz z-scan rate allows sufficient time for effective antigen–antibody binding on the cell membrane,^{26,30} and thus the probed forces adequately reflect the protein distribution.

An affinity map contains all of the information needed for quantifying local protein expression. To count the proteins accurately, the tip dimension must match the pixel size when the antibody modified tip scans across the membrane. Otherwise, some surface proteins may be either ignored or addressed multiple times. According to the SEM images of a gold-coated probe (radius of tip apex is $\sim 42 \text{ nm}$) and according to the dimensions of the cross-linker SPDP ($\sim 0.7 \text{ nm}$ in length) and IgG ($16\text{--}19 \text{ nm}$ in length),³¹ the diameter of the tip contact area is $\sim 120 \text{ nm}$, which correlates to approximately one pixel (125 nm) in a $4 \times 4 \mu\text{m}^2$ affinity map. Thus, a $4 \times 4 \mu\text{m}^2$ affinity map suits our purpose of analyzing the protein distribution. However, this scale will vary based on the dimensions of the tip and the ligand in other studies.

Quantitative analysis of protein expression relies on the determination of the specific binding force between a single antigen–antibody pair above the nonspecific interaction level. To evaluate the nonspecific interaction level, we modified the AFM tip with PEG, a cell resistant polymer. Due to the lack of

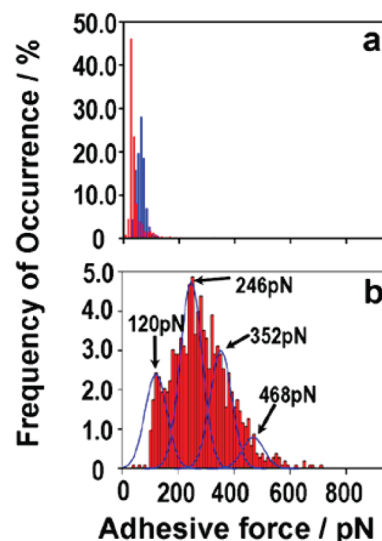


Figure 2. Probability histograms of unbinding forces summarized from (a) $4 \times 4 \mu\text{m}^2$ affinity maps collected by a PEG modified tip on undifferentiated cells (blue columns) and by an anti-E-cadherin modified tip on undifferentiated cells preincubated in culture media containing 1% BSA for 1 h, followed by incubation in media containing $10 \mu\text{g}/\text{mL}$ of anti-E-cadherin for 2.5 h (red columns) and (b) a $1 \times 1 \mu\text{m}^2$ affinity map collected by an anti-E-cadherin modified tip on an undifferentiated cell. The histogram is fitted by a Gaussian (bars, experimental data; solid lines, Gaussian fitting curves).

specific interaction, any force addressed by this tip on a cell is ascribed to nonspecific interactions, arising from tip convolution, cell surface roughness, and the weak interaction of PEG with various cell surface species. As shown in the histogram in Figure 2a (blue columns), the most probable force appears at 60–70 pN, and 94% of measured forces are below 90 pN. In a separate control experiment, we incubated the cells in culture media containing 1% BSA for 1 h, followed by incubation in media containing $10 \mu\text{g}/\text{mL}$ of anti-E-cadherin (four times higher than the concentration used for immunostaining) for 2.5 h to inhibit binding of anti-E-cadherin on the tip to E-cadherin on the cell membrane. As shown in the histogram in Figure 2a (red columns), which summarizes the force maps collected from five different cells from two different cultures, strong adhesion forces were largely abrogated with the most probable force appearing at 20–30 pN, with 93% of measured forces below 90 pN. We also used an anti-E-cadherin modified tip to collect $1 \times 1 \mu\text{m}^2$ affinity maps on a hES cell, where the level of nonspecific interaction was greatly diminished with the decrease in image size due to the relatively smooth surface and the lack of complicated cell surface species within small areas of a cell.²⁷ The results are summarized in the histogram in Figure 2b. A negligible number of adhesion forces are below 90 pN. The combined data allow us to conclude that the level of nonspecific interaction is less than 90 pN. By Gaussian fitting, we identified four peaks in the histogram, corresponding to 120, 246, 352, and 468 pN, respectively, which appear to be integer multiples of a quanta unit $120 \pm 10 \text{ pN}$. Thus, we infer $120 \pm 10 \text{ pN}$ as the force of a single-pair antigen–antibody interaction, consistent with previous results reported in the literature³² as well as in our previous report.²⁷ On the basis of this value, we can quantify the E-cadherin density, i.e., the number of proteins per unit area, by integrating the areas below the fitting curves as delineated below.

Quantification of Protein Expression on a Target Cell. To establish the *in situ* single-cell protein quantification, we carried out an immunofluorescence analysis of E-cadherin expression

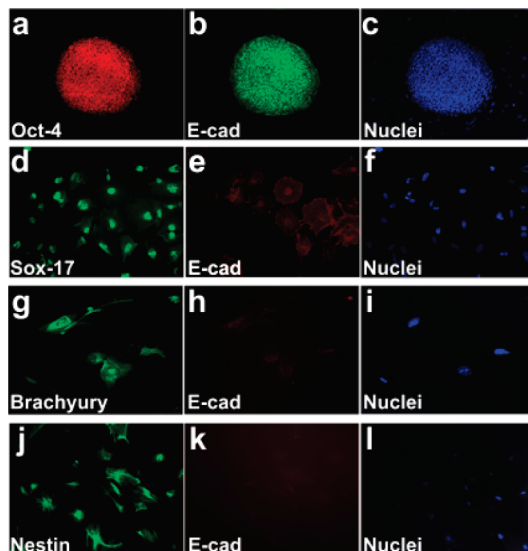


Figure 3. Immunofluorescence analysis of hES cells. (a–c) Double-immunostaining of undifferentiated hES cells for Oct-4 and E-cadherin. Double-immunostaining of spontaneously differentiated cells at day 13: (d–f) endoderm lineage for Sox-17 and E-cadherin; (g–i) mesoderm lineage for brachyury and E-cadherin; (j–l) ectoderm lineage for nestin and E-cadherin. Nuclei were stained with DAPI.

on hES cells for reference. As shown in Figure 3, undifferentiated hES cells form round-shaped colonies with clear boundaries. Oct-4 gene expression is characteristic for undifferentiated pluripotent hES cells. Cells within a colony were strongly positive for both Oct-4 (Figure 3a) and E-cadherin (Figure 3b), whereas those departing from a colony after long-term culture expressed Oct-4 and E-cadherin at a decreased level, evidence of cell differentiation. After 13 days spontaneous differentiation, cells in different lineages were identified and examined. Sox-17 positive cells (Figure 3d) are round or polygonal in shape, form small clusters, and are well spread on the substrate, features characteristic for endoderm cells; they express E-cadherin at a lower level when compared with undifferentiated cells. Brachyury positive cells (Figure 3g) are elongated and show a spindle shape, typical for mesoderm cells; the E-cadherin expression level dropped dramatically on these cells. Nestin positive cells (Figure 3j) are cells in the ectoderm lineage, exhibiting an increasingly branched, filopodia-rich morphology, a phenotype of neural progenitor cells; these cells are mostly isolated, and their E-cadherin expression level is low. With the data normalized to that of an internal protein β -actin, the results of Western blot analysis indicated the level of E-cadherin protein decreased 3.8 ± 0.7 -fold upon the spontaneous differentiation of hES cells (on day 13). Taken together, E-cadherin expression is high on undifferentiated hES cells, whereas the expression level drops on differentiated cells. However, the degree of difference in E-cadherin expression level in cells of different lineage cannot be accurately evaluated due to the overall low abundance of E-cadherin in these cells.

The IF-AM method is unique in its ability to study protein expression level on a cell in a complex cell mixture. Spontaneously differentiated hES cells comprise a mixture of cells from different lineages. With the marker proteins providing the guidance, we probed the E-cadherin expression on lineage specific cells using an anti-E-cadherin modified AFM tip (Figure 4). The histograms are summarized from multiple $4 \times 4 \mu\text{m}^2$ affinity maps of the target cells at random locations. Among the cells of the three lineages, ectoderm (nestin positive) cells show more than 81.4% of the collected forces below 90 pN,

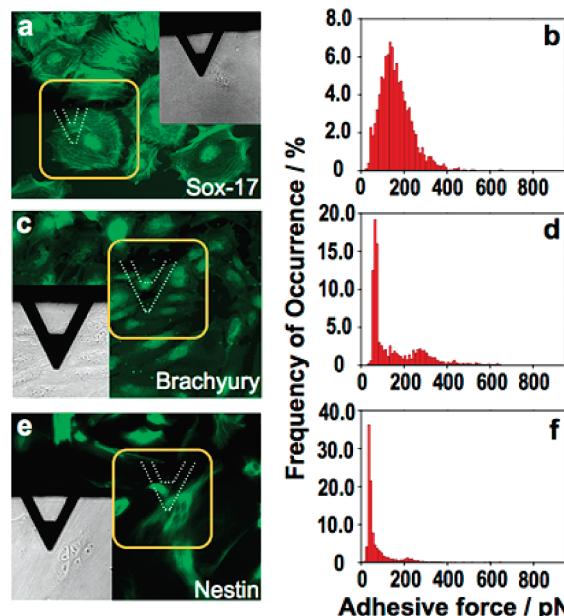


Figure 4. IF-AM study of E-cadherin expression on cells at day 13 of spontaneous differentiation. Anti-E-cadherin modified tips (the shape indicated by white dots) were positioned on a Sox-17 positive cell (a), a brachyury positive cell (c), and a nestin positive cell (e), respectively. Insets of (a,c,e) are the phase images showing the tip position on a target cell. (b,d,f) Corresponding histograms from $4 \times 4 \mu\text{m}^2$ affinity maps collected on Sox-17 positive cells (b), brachyury positive cells (d), and nestin positive cells (f), respectively.

TABLE 1: E-Cadherin Protein Density on Various Cells

cell type	undifferentiated hES cells		cells on day 13 of differentiation		
	junction	center	endoderm	mesoderm	ectoderm
E-cadherin number/ μm^2	196 ± 21	204 ± 25	85 ± 5	42 ± 4	11 ± 4

the nonspecific interaction level. In mesoderm (brachyury positive) cells, the most probable adhesion force appears at 70 pN, and more than 51.4% of the forces are below 90 pN. The endoderm (sox-17 positive) cells show a higher degree of adhesion forces; however, the most probable adhesion forces are in the range of 110–150 pN, and only a few adhesion forces were measured above 300 pN. By Gaussian fitting of the histograms and integration of the fitting curves, as well as the identification of 120 pN as the force of a single antigen–antibody interaction, we estimated the protein densities are 11 ± 4 , 42 ± 4 , and 85 ± 5 proteins/ μm^2 on the examined ectoderm, mesoderm, and endoderm lineage cells, respectively (Table 1). The protein densities were derived from 3 to 5 different cells in at least two different cultures. In contrast, the E-cadherin expression on the undifferentiated cells is averaged at 202 ± 27 proteins/ μm^2 among the 12 different cells in five different cultures. This quantity of E-cadherin expression is at the same level as the average E-cadherin per cell reported by Foyt et al. using quantitative flow cytometry.³³ These data are consistent with the qualitative results from immunofluorescence imaging, and any protein expression disparity among cells of different lineages is well resolved despite the low abundance of E-cadherin.

Quantification of Local Protein Density at the Subcellular Level. A singular advantage of the IF-AM method is the ability to quantify the local protein expression of a cell due to the high lateral resolution of AFM. As shown in Figure 5a and b, an anti-E-cadherin modified AFM tip can be selectively positioned

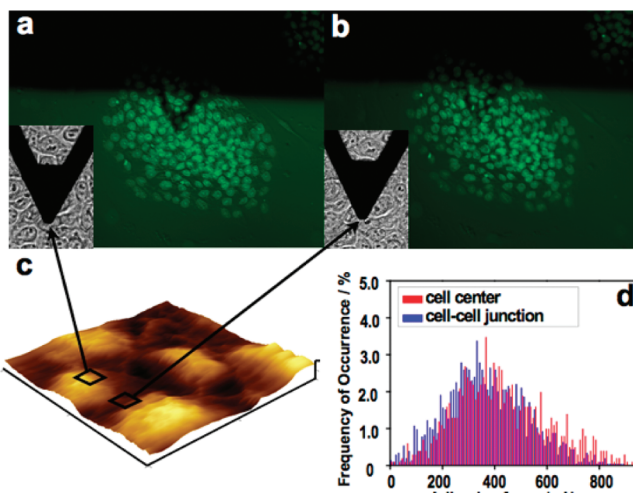


Figure 5. IF-AM study of E-cadherin local expression on a hES cell. (a,b) Immunofluorescent images (staining with the antibody against Oct-4) of an undifferentiated hES cell colony grown on a cell culture dish, showing the tip was selectively positioned at the cell center (a) and the cell junction (b), respectively. Insets are the phase images indicating the tip position. These local regions are also highlighted in the 3D AFM image (c) of the same cell colony. The AFM image size is $32 \times 32 \mu\text{m}^2$; the z-scale bar is $4 \mu\text{m}$. (d) Probability histograms of unbinding forces summarized from $4 \times 4 \mu\text{m}^2$ affinity maps collected at the cell centers (red) and cell junctions (blue) using anti-E-cadherin modified tips.

at the center (or nonjunction area) of an Oct-4 positive cell or the junction of adjacent cells, as clearly visualized in the 3D large scale AFM image in Figure 5c. Figure 5d shows the histograms derived from $4 \times 4 \mu\text{m}^2$ affinity maps of six hES cells in four separate cell cultures collected at the cell centers and at the cell junctions, respectively. The histograms indicate that the observed adhesion forces slightly shift to the high-force range at the cell center vs the cell junction. Similar to the aforementioned method, we estimated the protein expressions as $204 \pm 25 \text{ proteins}/\mu\text{m}^2$ at the cell center and $196 \pm 21 \text{ proteins}/\mu\text{m}^2$ at the cell junction, respectively (Table 1). When repeatedly measured on the same cell and different cells, the protein density at the cell center was typically higher by 4–12 $\text{proteins}/\mu\text{m}^2$ than at the cell junction. This implies that the E-cadherin expression level is comparable or even higher at the cell center than that at the cell junction on the membrane of hES cells within at least our culture.

With an affinity map, we essayed to analyze the homogeneity of protein distribution on a cell. E-Cadherin is a 120 kD protein and has a typical size of $\sim 24 \text{ nm}$ in diameter.³⁴ On the basis of the protein density of $202 \pm 27 \text{ proteins}/\mu\text{m}^2$ on undifferentiated cells, the center–center distance of neighboring proteins was estimated at an average 70 nm. Since the affinity maps were collected by an antibody-modified tip with an apex diameter of $\sim 120 \text{ nm}$, and the dimension of a pixel in a $4 \times 4 \mu\text{m}^2$ affinity map (32 pixels per line) is 125 nm, it is expected that the tip would address E-cadherin proteins at each pixel if the protein distribution is homogeneous. This is confirmed by the fact that low-adhesion ($< 90 \text{ pN}$, the cutoff of nonspecific interaction) force occurrence, i.e., the frequency of observing E-cadherin unoccupied pixels, in an undifferentiated cell is below 1.6% for cell centers and 2.3% for cell junctions in the histograms (Figure 5a). Additionally, the low-force pixels are randomly distributed on the affinity maps (see Figure 1c), suggesting a relatively homogeneous distribution of E-cadherin regardless of its high density on the cell membrane. For comparison, we

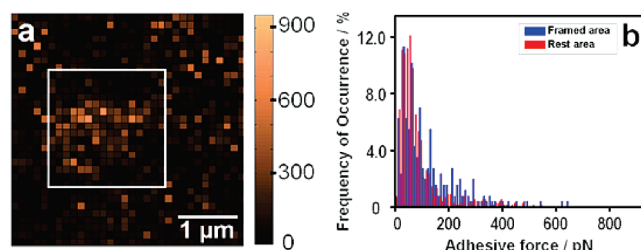


Figure 6. Measurement of TRA-1-81 local distribution on an undifferentiated hES cell. (a) A $4 \times 4 \mu\text{m}^2$ affinity map reconstructed from a total of 1024 force curves that were collected using an anti-TRA-1-81 modified AFM tip. The framed area is a region with high TRA-1-81 expression. (b) Probability histograms of unbinding forces summarized from the pixels at the highlighted region (blue) and the remaining region (red).

also examined the distribution of another membrane protein, TRA-1-81. A $4 \times 4 \mu\text{m}^2$ affinity map collected on an undifferentiated hES cell is shown in Figure 6a. When compared with the affinity map in Figure 1c, Figure 6a is darker in general, suggesting a lower TRA-1-81 expression level. The framed region shows the brightest contrast on the map, indicating the localization of TRA-1-81. The high-force regions are highly localized and are apparently segregated by low-force regions, suggesting the heterogeneous distribution of TRA-1-81 on the hES cell. The heterogeneity was observed repeatedly on multiple undifferentiated cells from different cultures.

The protein local expression pattern was confirmed by further quantitative analysis. If we equally divide the affinity map in Figure 1c into four regions (indicated in the figure), the E-cadherin density is estimated at 203, 177, 175, and 190 $\text{proteins}/\mu\text{m}^2$, respectively, which is consistent with the relatively homogeneous distribution of E-cadherin. In contrast, with the histograms (Figure 6b) summarized from the affinity map in Figure 6a, we calculated that the TRA-1-81 densities are 83 $\text{proteins}/\mu\text{m}^2$ at the highlighted area and 28 $\text{proteins}/\mu\text{m}^2$ at the remaining region, evidence of a heterogeneous protein distribution. Note that homogeneous distribution of TRA-1-81 is characteristic for initially differentiated cells²⁷ accompanied by a decline of the protein expression level.

Discussion

With the guidance provided by a fluorescence probe and the high lateral resolution of AFM, we attempted the quantification of protein density on a target cell within a cell mixture and spatially resolved the local protein expression at the subcellular level. The advantages of this IF-AM method are 3-fold: (1) quantification of protein density allows the detection of subtle differences in protein expression among the cells with low protein abundance at high sensitivity; (2) protein quantification can be performed on-site, making the method a potential tool for studying the dynamics of protein reorganization during cell development; (3) the method is sensitive enough to probe the difference in the local expression of proteins on a target cell.

The information derived from the quantitative method helps us understand the effect of the cellular environment in hES cell fate. Though the function of TRA-1-81 in hES cells is unknown, the fact that the distribution of TRA-1-81 is heterogeneous on an undifferentiated cell and homogeneous on an initially differentiated cell suggests the distribution pattern of TRA-1-81 can be used as a physical marker in identifying the hES cell status.²⁷ E-Cadherin is located on surfaces of cells in regions of cell–cell contact known as adherens junctions. This is consistent with the observation that E-cadherin is highly

populated at the cell junction in many adhesive and well-spreading cells.³⁵ However, our measurements reproducibly indicate that E-cadherin expression at the cell center is comparable or higher than that at the cell junction of undifferentiated hES cells. We interpret such a unique E-cadherin distribution by the capability of hES cells recruiting additional cells on top to grow in multilayers, a common feature of hES cell colonies. When the hES cells are differentiated, E-cadherin expression is 2- to 16-fold lower, depending on the cell lineage (Table 1). The results imply that E-cadherin mediated cell–cell interaction plays a crucial role in maintaining the “stemness” of hES cells. E-Cadherin not only provides the cell–cell adhesion to “glue” the cells but also balances the β -catenin expression at the cell membrane and at the nuclei via the binding of β -catenin with its intracellular domain at an adherens junction.^{36–39} Membrane-uncomplexed β -catenin has a function of transducing the Wnt signal from the cell surface to the nucleus.^{38,40–42} The high expression of E-cadherin at the surface of undifferentiated cells may impede the accumulation of β -catenin at the nuclei, thus prohibiting the transcription of Wnt responsive genes which promote hES cell differentiation. This hypothesis is supported by the results from our recent immunofluorescence images, which clearly showed that β -catenin largely remained in the cytoplasm of undifferentiated hES cells, whereas it relocated to the nuclei upon hES cell differentiation. The reduced E-cadherin level on differentiated hES cells was also observed by D’Amour et al. when they differentiated hES cells to endoderm cells.⁴³

The research marked the initial effort in developing a precise quantification method for on-site protein analysis at the single cell level. More efforts are needed to improve the accuracy of protein abundance quantification. For instance, in our study, protein distribution was resolved at a single pixel level, e.g., an area of $125 \times 125 \text{ nm}^2$ in a $4 \times 4 \mu\text{m}^2$ affinity map, instead of at the single protein level. Though the number of pixels per map can be increased and the scale of affinity maps can be decreased, due to the mismatch of the pixel size and the probe dimension, these maps are not eligible for analyzing the protein distribution in the current study. This problem can be tackled by reducing the dimension of the modified probe, which can be achieved by reducing the dimension of the tip apex or by modifying the antibodies within a constrained small area of a tip. The latter may be a better choice as a sharp tip can easily indent and penetrate a cell membrane, which complicates the adhesion force measurements.

In this study, we applied the maximum adhesion force to the quantification of specific interactions that were utilized to count the number of proteins at local regions. Counting of the number of proteins relies on the fitting of the histograms. Gaussian distribution was applied in the fitting in reference to other AFM studies of antigen–antibody interactions,^{17,30,44} though a more comprehensive fitting method can lead to more accurate quantification. Strong adhesion forces corresponding to multiple bond formation were frequently observed. The use of maximum adhesion force is simple and straightforward. However, it has the disadvantage of skipping some of the binding features reflected on a force curve; the assumed linear relationship between the maximum adhesion force and the number of protein is a highly simplified model. Ikai et al. suggested the use of separation work, based on the area under the force-extension curve, to measure the specific interaction.^{13,14} Separation work reflects the overall adhesion strength in the contact area and thus is a better measure of multiple bonds in quantifying protein density. We expect to adapt the separation work based calcula-

tion in our future work to improve the accuracy of protein quantification.

A unique feature of the IF-AM method is the ability to perform on-site analysis of surface protein distribution on a target cell. A significant drawback of the method at the current stage, however, is the slow process of force measurement by an AFM, which hinders its throughput in dynamic studies of cells at different status and in various stages during the development. The recent advancement in fast scanning AFM is expected to provide a promising solution to this issue.

Conclusion

We established the IF-AM method which marked the initial effort to develop a precise quantification method for on-site analysis of proteins at both high and low abundance. The spatially resolved quantitative method provided a platform for understanding the correlation between hES cell stemness and the unique colony growth pattern mediated by E-cadherin. With improvements, the method is expected to be applied for quantitative analysis of any cell membrane protein expression at a desired area of a target cell. Modification of the method is under way to achieve spatially resolved information concerning protein–protein association among the same and different protein species to reveal the protein reorganization in response to ligand binding.

Acknowledgment. This research was supported by NIH (R01 NS047719) and a seed grant from the Pritzker Institute of Biomedical Science and Engineering at IIT. We thank Prof. Tom Irving for critical reading of this manuscript.

References and Notes

- (1) Kwon, O.; Myers, B. D.; Sibley, R.; Dafoe, D.; Alfrey, E.; Nelson, W. J. *J. Histochem. Cytochem.* **1998**, *46*, 1423.
- (2) Mayhew, T. M.; Mählfeld, C.; Vanhecke, D.; Ochs, M. *Ann. Anat.* **2009**, *191*, 153.
- (3) Cherry, R. J.; Morrison, I. E. G.; Karakikes, I.; Barber, R. E.; Silkstone, G.; Fernández, N. *Biochem. Soc. Trans.* **2003**, *31*, 1028.
- (4) Davey, H.; Kell, D. *Microbiol. Rev.* **1996**, *60*, 641.
- (5) Ahmad, M. C.; Lewis, A. C.; Gillies, W. M.; Ruth, J. M. *Oncogene* **2002**, *21*, 9.
- (6) Chiang, L. W. *J. Chromatogr. A* **1998**, *806*, 209.
- (7) Audinat, E.; Lambolez, B.; Rossier, J. *J. Neurochem. Int.* **1996**, *28*, 119.
- (8) Emmert-Buck, M. R.; Bonner, R. F.; Smith, P. D.; Chuaqui, R. F.; Zhuang, Z.; Goldstein, S. R.; Weiss, R. A.; Liotta, L. A. *Science* **1996**, *274*, 998.
- (9) Wang, K.; Lau, T. Y.; Morales, M.; Mont, E. K.; Straus, S. E. *J. Virol.* **2005**, *79*, 14079.
- (10) Bhushan, B.; Fuchs, H. O. *Applied scanning probe methods III: Characterization*, 1st ed.; Springer-Verlag: Berlin, 2006; pp 1–24.
- (11) Junker, J. P.; Rief, M. *Proc. Natl. Acad. Sci. U.S.A.* **2009**, *106*, 14361.
- (12) Stroh, C.; Wang, H.; Bash, R.; Ashcroft, B.; Nelson, J.; Gruber, H.; Lohr, D.; Lindsay, S. M.; Hinterdorfer, P. *Proc. Natl. Acad. Sci. U.S.A.* **2004**, *101*, 12503.
- (13) Kim, H.; Arakawa, H.; Hatae, N.; Sugimoto, Y.; Matsumoto, O.; Osada, T.; Ichikawa, A.; Ikai, A. *Ultramicroscopy* **2006**, *106*, 652.
- (14) Kim, H.; Arakawa, H.; Osada, T.; Ikai, A. *Ultramicroscopy* **2003**, *97*, 359.
- (15) Hoh, J. H.; Cleveland, J. P.; Prater, C. B.; Revel, J. P.; Hansma, P. K. *J. Am. Chem. Soc.* **1992**, *114*, 4917.
- (16) Reddy, C. V. G.; Malinowska, K.; Menhart, N.; Wang, R. *Biochim. Biophys. Acta, Biomembr.* **2004**, *1667*, 15.
- (17) Yu, J.; Wang, Q.; Shi, X.; Ma, X.; Yang, H.; Chen, Y.-G.; Fang, X. *J. Phys. Chem. B* **2007**, *111*, 13619.
- (18) Henderson, E.; Sakaguchi, D. S. *NeuroImage* **1993**, *1*, 145.
- (19) Poole, K.; Muller, D. *Br. J. Cancer* **2005**, *92*, 1499.
- (20) Thomson, J. A.; Itskovitz-Eldor, J.; Shapiro, S. S.; Waknitz, M. A.; Swiergiel, J. J.; Marshall, V. S.; Jones, J. M. *Science* **1998**, *282*, 1145.
- (21) Yu, J.; Thomson, J. A. *Genes Dev.* **2008**, *22*, 1987.
- (22) Sridharan, I.; Kim, T.; Wang, R. *Biochem. Biophys. Res. Commun.* **2009**, *381*, 508.

- (23) Schwartz, M. A.; DeSimone, D. W. *Curr. Opin. Cell Biol.* **2008**, *20*, 551.
- (24) Wells, A.; Yates, C.; Shepard, C. *Clin. Exp. Metastasis* **2008**, *25*, 621.
- (25) Yap, A. S.; Crampton, M. S.; Hardin, J. *Curr. Opin. Cell Biol.* **2007**, *19*, 508.
- (26) Vengasandra, S.; Sethumadhavan, G.; Yan, F.; Wang, R. *Langmuir* **2003**, *19*, 10940.
- (27) Qiu, D.; Xiang, J.; Li, Z.; Krishnamoorthy, A.; Chen, L.; Wang, R. *Biochem. Biophys. Res. Commun.* **2008**, *369*, 735.
- (28) Tang, Q.; Zhang, Y.; Chen, L.; Yan, F.; Wang, R. *Nanotechnology* **2005**, *16*, 7.
- (29) Tortonese, M.; Kirk, M. *Characterization of application-specific probes for SPMs*; Micromachining and Imaging, San Jose, CA, USA, 1997.
- (30) Hinterdorfer, P.; Baumgartner, W.; Gruber, H. J.; Schilcher, K.; Schindler, H. *Proc. Natl. Acad. Sci. U.S.A.* **1996**, *93*, 3477.
- (31) Roberts, C. J.; Williams, P. M.; Davies, J.; Dawkes, A. C.; Sefton, J.; Edwards, J. C.; Haymes, A. G.; Bestwick, C.; Davies, M. C.; Tendler, S. J. B. *Langmuir* **1995**, *11*, 1822.
- (32) Alessandrini, A.; Facci, P. *Meas. Sci. Technol.* **2005**, *16*, 65.
- (33) Foty, R. A.; Steinberg, M. S. *Dev. Biol.* **2005**, *278*, 255.
- (34) Miyaguchi, K. *J. Struct. Biol.* **2000**, *132*, 169.
- (35) Takeichi, M. *Science* **1991**, *251*, 1451.
- (36) Aberle, H.; Butz, S.; Stappert, J.; Weissig, H.; Kemler, R.; Hoschutzky, H. *J. Cell Sci.* **1994**, *107*, 3655.
- (37) Jou, T. S.; Stewart, D. B.; Stappert, J.; Nelson, W. J.; Marrs, J. A. *Proc. Natl. Acad. Sci. U.S.A.* **1995**, *92*, 5067.
- (38) Orsulic, S.; Huber, O.; Aberle, H.; Arnold, S.; Kemler, R. *J. Cell Sci.* **1999**, *112*, 1237.
- (39) Hülsken, J.; Behrens, J.; Birchmeier, W. *Curr. Opin. Cell Biol.* **1994**, *6*, 711.
- (40) Moore, K. A.; Lemischka, I. R. *Science* **2006**, *311*, 1880.
- (41) Li, L.; Neaves, W. B. *Cancer Res.* **2006**, *66*, 4553.
- (42) Fuchs, E.; Tumbar, T.; Guasch, G. *Cell* **2004**, *116*, 769.
- (43) D'Amour, K.; Agulnick, A.; Eliazer, S.; Kelly, O.; Kroon, E.; Baetge, E. *Nat. Biotechnol.* **2005**, *23*, 1534.
- (44) Dupres, V.; Menozzi, F. D.; Locht, C.; Clare, B. H.; Abbott, N. L.; Cuenot, S.; Bompard, C.; Raze, D. J.; Dufrene, Y. F. *Nat. Meth* **2005**, *2*, 515.

JP906737Q